Energy-Dispersive XAFS Studies on the Spontaneous Dispersion of PdO and the Formation of Stable Pd Clusters in Zeolites

Kazu Okumura,*,† Ryosuke Yoshimoto,† Tomoya Uruga,‡ Hajime Tanida,‡ Kazuo Kato,‡ Shigeru Yokota,‡ and Miki Niwa†

Department of Materials Science, Faculty of Engineering, Tottori University, Koyama-cho, Tottori 680-8552, Japan, and Japan Synchrotron Radiation Research Institute, 1-1-1 Kouto, Mikazuki-cho, Sayo-gun, Hyogo 679-5198, Japan

Received: October 21, 2003; In Final Form: March 17, 2004

Spontaneous dispersion and clustering processes of Pd were measured by means of the energy-dispersive EXAFS method. The spontaneous dispersion of bulky metal Pd into highly dispersed PdO was directly observed on the H-type zeolite in the atmosphere of O_2. In contrast to H-type zeolites, simple oxidation of the agglomerated Pd was observed on Na−ZSM-5. The structural change of Pd was followed in the atmosphere of hydrogen. The clustering processes of metal Pd depended on the kind of zeolite, and these were categorized into three groups. The first group, i.e., Na−ZSM-5 and H−β, showed monotonic agglomeration of metal Pd by increasing the reduction temperature. The second group consisted of H−ZSM-5 and H−mordenite where the formation of Pd_6 clusters was found. On these zeolites, the generation of Pd_6 clusters was reversibly observed upon the repetition of reduction and oxidation treatments. The third group consisted of H−Y and USY zeolites where the formation of Pd_{13} clusters was observed. From these findings, it was concluded that the crystal structure and acid sites of zeolites had profound influences on the dynamic behavior and the genesis of Pd clusters with various structures.

1. Introduction

Small metal clusters occluded in a zeolite pore have been studied primarily from the viewpoint of the formation of uniform active sites for catalytic reactions. The introduction of metals in zeolites has been achieved through various techniques including CVD (chemical vapor deposition), ship-in-bottle method, and decarbonylation of carbonyl clusters in zeolite pores.[1−5] Particularly, palladium clusters in zeolites have been given attention since Pd exhibited high catalytic activities in many kinds of valuable reactions, such as selective reduction of NO, total combustion of hydrocarbons, and organic reactions.[6−9] Recently, small metal Pd clusters were obtained through the introduction of Pd in the pore of Na−Y zeolite, followed by a successive reduction at low temperatures. In addition, it was found that the location of the metal Pd cluster in X- and Y-zeolites was significantly affected by the calcination temperature.[10,11] In the present study, we have focused on the influence of the Brønsted acid site as well as the structure of zeolite on the generation of metal Pd clusters and highly dispersed PdO. This is because it has been revealed that the structure and the acid sites of zeolites considerably affected the generation of active sites for catalytic reactions. As a matter of fact, the catalytic performance of Pd was greatly dependent on the structure and composition of zeolite supports. The fact suggested that the strong metal−support interaction between PdO and Brønsted acid sites was an important factor in not only the generation but also the catalytic performance of an active Pd center. The interaction was directly evidenced from the structural change of Pd induced by the Brønsted acid site of zeolites in the oxidative or reductive atmosphere. Namely, we have found that the agglomerated metal Pd spontaneously migrated into zeolite pores to become the molecular-like dispersed PdO on acid sites of ZSM-5 and mordenite-type zeolites under O_2 atmosphere at elevated temperatures.[12−15] Furthermore, this spontaneous dispersion of PdO was reversible upon a repetition of reduction and oxidation treatment as proved by the precise EXAFS measurements. From these findings, it was postulated that the Brønsted acid sites played a key role in the generation of metal Pd clusters. To further understand the dynamic behavior of Pd with zeolite supports, we have tried to measure the local structure of Pd during the dispersion and clustering process of metal Pd in H-form zeolites. The dispersion process of Pd was followed by using H−ZSM-5 and H−mordenite as supports. Comparable experiments were performed using Na−ZSM-5 having no acid sites in order to make clear the effect of acid sites on the dispersion of PdO species. On the other hand, six kinds of zeolites, namely, H−ZSM-5, Na−ZSM-5, H−mordenite, H−β, H−Y, and USY, were employed as supports for Pd in the investigation of the influence of the structure and the kinds of cations on the generation of metal Pd clusters in zeolite pore. For these purposes, in situ energy-dispersive EXAFS (DXAFS) experiment was applied to the determination of the Pd structure during temperature-programmed heating in the atmosphere of O_2 and H_2. DXAFS is a powerful tool for studying dynamic structural changes of materials in real time. Using this method, it becomes possible to measure the structure of metals within a few seconds precisely.[16,17] The technique is particularly suitable for characterization of such Pd species generated inside the pore of zeolites, which is otherwise difficult to study. This is because a small amount of diluted Pd (0.4 wt %) was dispersed in zeolite matrix. In addition, in these samples the absorption of X-ray in

* Corresponding author. E-mail: okmr@chem.tottori-u.ac.jp.
† Tottori University.
‡ Japan Synchrotron Radiation Research Institute.

10.1021/jp037187b CCC: $27.50
Published on Web 04/23/2004

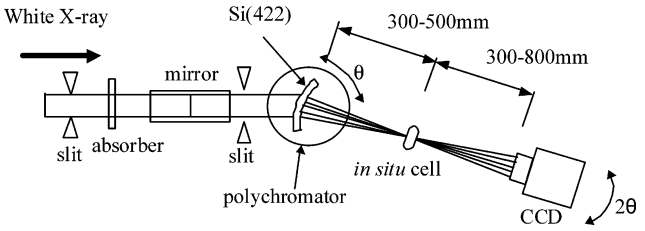

Figure 1. The schematic diagram of in situ DXAFS measurement at BL28B2 station in SPring-8.

zeolite is small in comparison with Pd at the energy region of Pd K-edge (24.3 keV). The fact enables the easiness of the collection of the data with high quality despite the low loading of Pd.

2. Experimental Section

Na−ZSM-5 ($Si/Al_2 = 23.8$), H−β ($Si/Al_2 = 25$), and USY ($Si/Al_2 = 7.51$) zeolites were supplied from Tosoh Co., PQ Corporation and Shokubai Kasei Co., respectively. H−mordenite (JRC-Z-HM15, JRC-ZM20), and HY (JRC-Z-HY5.5) zeolites were supplied from The Catalysis Society of Japan. H−ZSM-5 was prepared through an ion-exchange method using Na−ZSM-5 and 0.5 M NH_4NO_3 solution, followed by calcination in N_2 at 773 K. Pd was loaded on these zeolites through an ion-exchange method using $Pd(NH_3)_4Cl_2$ solution. An amount of 0.4 wt % of Pd was loaded on each zeolite. The samples were calcined in an N_2 flow at 773 K for 4 h prior to the measurements.

Pd K-edge DXAFS was measured at BL28B2 station of Japan Synchrotron Radiation Research Institute (SPring-8).[18] The storage ring of SPring-8 was operated at 8 GeV. The schematic arrangement of the DXAFS measurement was given in Figure 1. The main equipment consists of a polychromator, a higher-harmonic-rejecting mirror, and a position-sensitive detector (PSD). The polychromator, sample, and PSD are mounted on a $\theta-2\theta$ diffractometor. White X-rays emanating from the bending magnet source are diffracted by a bent crystal in the polychromator and focused on the sample. For the measurements of Pd K-edge, the Si polychromator crystal was switched to a Laue configuration with (422) net plane to obtain the X-ray beam with dispersed energy region. The diffracted X-rays possess differing energies, depending on the diffraction angle. The X-rays are measured with the PSD at the position corresponding to their energy. The energy resolution at Pd K-edge was estimated to be 3 eV. The energy of X-ray was calibrated using Pd foil as a reference. In the in situ measurement, a wafer form of the sample was placed in a quartz cell. The thickness of the sample was 1.5 cm to give the edge jump of 0.2. In practice, 8 pieces of sample disk (60 mg per disk) were placed in the quartz holder. The sample was heated from room temperature to 773 K with a ramp rate of 5 K min^{-1} in a pure O_2 flow (flow rate: 50 mL min^{-1}) or an 8% H_2 flow diluted with He (total flow rate: 100 mL min^{-1}) at atmospheric pressure. The spectra measured for 0.1−0.3 s were accumulated 10 times in every 10 K. Examples of raw spectra for Pd/H−ZSM-5 measured during temperature-programmed oxidation were given in Figure 2. It could be confirmed that fairly good spectra were obtained despite the low loading of Pd (0.4 wt %). For extended X-ray absorption fine structure (EXAFS) analysis, the oscillation was extracted by a spline smoothing method. The oscillation was normalized by edge height around 50 eV above the threshold. The Fourier transformation of the k^3-weighted EXAFS oscillation from k space to r space was performed over the range 20−110 nm^{-1} to obtain a radial distribution function. The inversely Fourier filtered data were analyzed with a curve-fitting method in the k range between 30 and 100 nm^{-1}.[19] For the curve-fitting analysis, the empirical phase shift and amplitude functions for nearest-neighbor Pd−Pd and Pd−O were extracted from the data for Pd foil and bulk PdO, respectively. In the analysis of spectra of DXAFS data of real samples, the Debye−Waller factors of Pd−O and nearest-neighboring Pd−Pd were extracted from the spectra of PdO and Pd powder measured at the same temperatures, respectively. The analysis of EXAFS data was performed using the "REX20 ver. 2.0.4" program (RIGAKU).

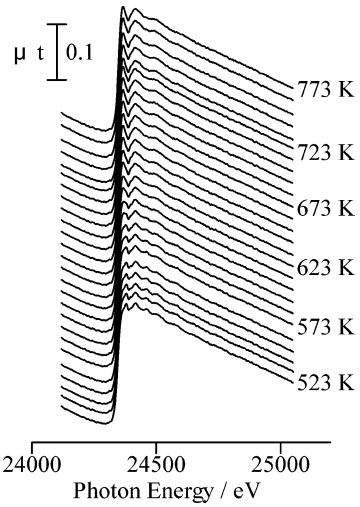

Figure 2. Pd K-edge XAFS spectra for Pd loaded on H−ZSM-5 ($Si/Al_2 = 23.8$) measured in an O_2 flow.

3. Results and Discussion

3.1. Spontaneous Dispersion of PdO onto Acid Sites of Zeolites. The changes in the structure of Pd loaded on Na−, H−ZSM-5, and H−mordenite were followed by the DXAFS in an atmosphere of oxygen. The samples were calcined at 773 K in an N_2 flow prior to the measurements. Fourier transforms of the $k^3\chi(k)$ EXAFS for Pd-loaded zeolites were given in Figure 3. Initially the formation of metal Pd was confirmed from the appearance of an intense nearest-neighboring Pd−Pd peak situated at 0.25 nm in every sample. From the coordination number of the Pd−Pd peak, the diameter of metal Pd was estimated to be larger than 1 nm in every sample.[20] In the case of Pd/Na−ZSM-5 (Figure 3a), the intensity of Pd−Pd (metal) gradually decreased, accompanied by raising the temperature in an oxygen flow. Alternatively, new peaks appeared at 0.15 and 0.32 nm. These peaks could be attributed to the Pd−O and Pd−(O)−Pd characteristic of agglomerated PdO from the comparison with the reference spectrum of bulk PdO. In the spectra of Pd/HZSM-5 (Figure 3b), the Pd−Pd peak steeply disappeared at 643 K. At the same time, the intensity of the Pd−O peak increased, indicating the oxidation of metal Pd progressed with raising the temperature. However, the Pd−(O)−Pd peak due to the agglomerated PdO did not appear. Although a similar feature was observed in Pd/H−mordenite (Figure 3c), it was observed that the temperature for the disappearance of Pd−Pd and the growth of Pd−O was higher than that of Pd/H−ZSM-5.

Figure 4 shows the coordination numbers (CN) of Pd−O, nearest-neighbor metal Pd−Pd, and Pd−(O)−Pd of Pd oxide plotted as a function of oxidation temperature. The CN values were calculated on the basis of the curve fitting analysis. As shown in Figure 4a, Pd−O and Pd−(O)−Pd peaks appeared in

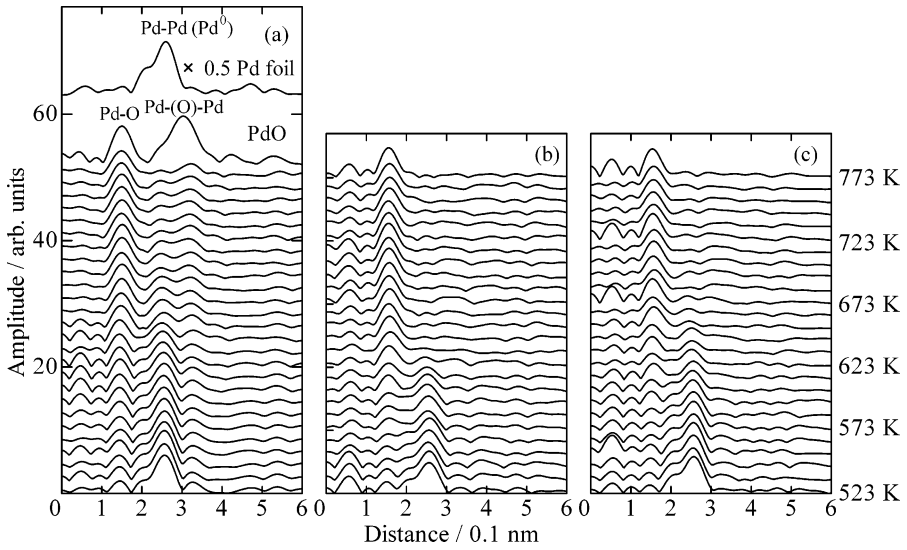

Figure 3. Pd K-edge EXAFS Fourier transforms for Pd loaded on (a) Na−ZSM-5, (b) H−ZSM-5, (c) H−mordenite measured in an O_2 flow; Pd loading, 0.4 wt %; temperature ramping rate, 5 K min^{-1}; the spectra of PdO and Pd foil were measured at room temperature.

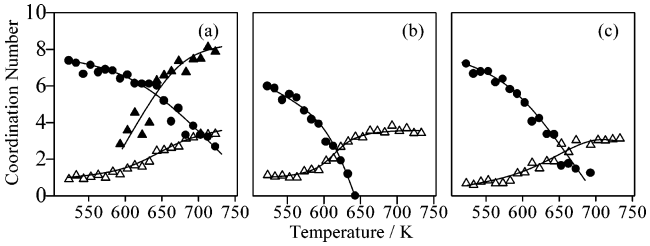

Figure 4. Dependence of coordination number on temperature measured in an O_2 flow for Pd loaded on (a) Na−ZSM-5, (b) H−ZSM-5, (c) H−mordenite. △ Pd−O, ● Pd−Pd (metal), ▲ Pd−(O)−Pd (oxide).

place of the decrease in Pd−Pd due to metal on Na−ZSM-5, accompanied by an increase in the temperature. The generation of the Pd−(O)−Pd meant that the metal Pd was simply transformed into the agglomerated PdO on the external surface of Na−ZSM-5 at elevated temperatures. On the H−ZSM-5 (Si/Al_2 = 23.8), the disappearance of the Pd−Pd peak and the growth of Pd−O were observed at 643 K. However, in contrast to the Na-form of ZSM-5, Pd−(O)−Pd peak did not appear even after the disappearance of metal Pd, which was characteristic of the agglomerated PdO. The fact meant that the agglomerated metal Pd migrated into the acid site of zeolite to generate highly dispersed PdO, because the size of PdO seemed to reflect on the intensity of the Pd−(O)−Pd shell. In addition, the data suggested that the migration of Pd took place immediately after the oxidation of metal Pd particle, since the oxidation and the dispersion of Pd were observed at the same time. Another dispersion process of PdO was revealed from the comparison with findings on H−ZSM-5 and Na−ZSM-5. Namely, the feature of transformation from metal Pd−Pd into Pd−O was sharp and the phenomenon occurred at a lower temperature over the H−ZSM-5 with respect to Na−ZSM-5. Taking the fact into account, it could be supposed that, in addition to spontaneous dispersion of PdO, the oxidation of metal Pd was promoted through the strong metal−support interaction between acid sites of H−ZSM-5 and PdO having basic character. The disappearance of metal Pd−Pd and the alternative growth of the Pd−O were accelerated over H−ZSM-5 with respect to on the H−mordenite. Thus it could be noted that the dispersion of Pd on ZSM-5 was easier than that of Pd/H−mordenite. Probably, the pore structure of zeolite or character of the acid center of zeolites affected the oxidation and migration process of Pd. Namely, probably the presence of the 3-dimensional pore system in ZSM-5 brought about a feasible migration of PdO in ZSM-5. The coordination number (4) and distance (0.202 nm) of Pd−O bond of highly dispersed PdO were closely similar to those of bulk PdO as reported already.

3.2. Formation of Metal Pd Clusters in Zeolite Pores with Different Structures. Figure 5 shows Fourier transforms of the $k^3\chi(k)$ EXAFS for Pd loaded on various kinds of zeolites measured during temperature-programmed reduction in an 8% H_2 flow. The samples were oxidized with O_2 at 773 K prior to the measurements. After the treatment, the formation of agglomerated PdO was observed in Na−ZSM-5, which was confirmed from the appearance of an intense Pd−(O)−Pd bond characteristic of bulk PdO at 0.29 nm. A similar spectrum was observed on the H−β zeolite (not shown). In contrast, the Pd−(O)−Pd peak did not appear on Pd/H−ZSM-5, H−mordenite, and H−Y. The fact indicated the generation of highly dispersed PdO on these zeolites, since the intensity of Pd−Pd shell seemed to reflect the size of PdO. Then, the pretreated samples were subjected to the temperature-programmed reduction with H_2 and the DXAFS measurements.

Figure 6 shows the coordination number (CN) of the nearest-neighboring Pd−Pd (metal Pd) peak determined on the basis of the curve-fitting analysis of the EXAFS spectra for Pd/Na−ZSM-5 and Pd/H−β. An intense Pd−Pd (metal) peak was observed from the beginning of the reduction, suggesting the generation of agglomerated metal Pd. From the CN of metal Pd−Pd, the diameter of metal Pd particle in Na−ZSM-5 reduced at 313 K was estimated to be 2 nm. Apparently, the size exceeded the pore diameter of Na−ZSM-5. Therefore, the generation of metal Pd particles was expected to occur on the external surface of Na−ZSM-5. The CN of Pd−Pd (metal) gradually increased from 8 to 10 with increasing the reduction temperature. This change pointed to the growth of metal Pd as it progressed, accompanied by raising the temperature. A similar change in the CN of Pd−Pd was observed on H−β zeolite. Thus it was concluded that the monotonic growth of metal Pd progressed on the external surface on these zeolites.

The features of Pd loaded on other zeolites were considerably different from that of Pd/Na−ZSM-5 and H−β. In the case of H−ZSM-5 and H−mordenite (Figure 7), a slight increase in the Pd−Pd was observed from the beginning of the reduction. At the same time, the CN of the Pd−O bond decreased,

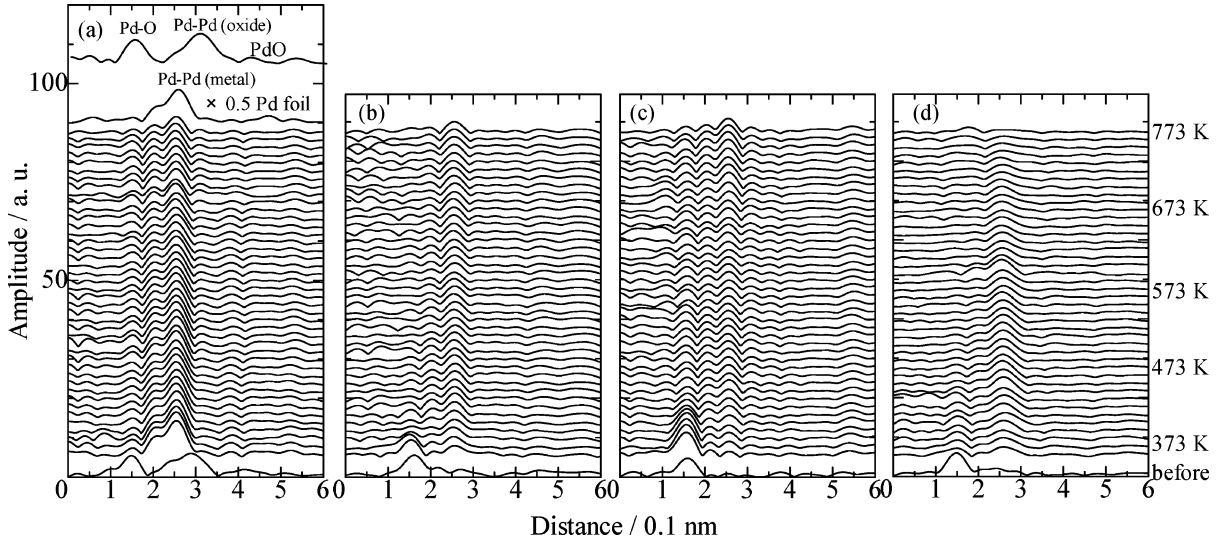

Figure 5. Pd K-edge EXAFS Fourier transforms measured during temperature-programmed reduction of (a) Pd/Na−ZSM-5, (b) Pd/H−ZSM-5, (c) Pd/H−mordenite, and (d) Pd/H−Y. The spectra of PdO and Pd foil were measured at room temperature.

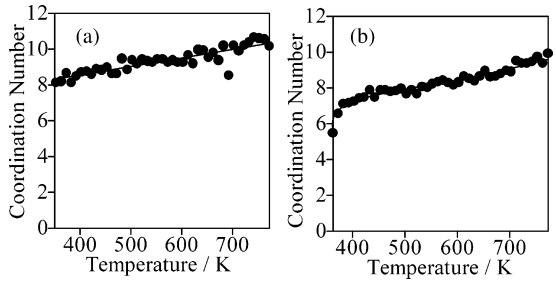

Figure 6. Dependence of coordination number of Pd−Pd (●) on the temperature measured in an 8% H_2 flow; (a) Pd/Na−ZSM-5 and (b) Pd/H−β.

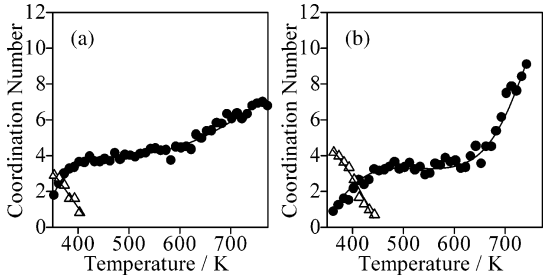

Figure 7. Dependence of coordination number of Pd−Pd (●) and Pd−O (△) on the temperature measured in an 8% H_2 flow; (a) Pd/H−ZSM-5 and (b) Pd/H−mordenite.

suggesting that the reduction of PdO to metal Pd took place up to 440 K. After the completion of the reduction, the CN of metal Pd−Pd kept a constant value at 4 between 430 and 620 K on both H−ZSM-5 and H−mordenite. It could be noted that the appearance of the plateau meant the generation of a stable Pd cluster at the temperature region. From the CN value, the Pd cluster was estimated to consist of 6 atoms. On further heating the samples under flowing H_2/He, the CN steeply increased from 620 to 770 K. Probably, the Pd_6 cluster migrated into the external surface of zeolites to form the agglomerated metal Pd particles. The change in CN on Pd/H−mordenite was similar to that on Pd/H−ZSM-5, except that the degree of growth of metal Pd observed above 620 K was steeper on H−mordenite.

After the measurements given in Figure 7, the samples were oxidized at 773 K for 4 h in an O_2 flow. Then the in situ cell was cooled to room temperature and the temperature-programmed reduction was carried out in an 8% H_2 flow again.

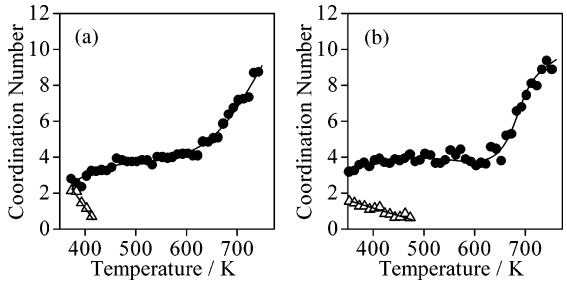

Figure 8. Dependence of coordination number of Pd−Pd (●) and Pd−O (△) during second run of temperature-programmed reduction in an 8% H_2 flow; The samples were pretreated with O_2 at 773 K after the measurement given in Figure 7; (a) Pd/H−ZSM-5 and (b) Pd/H−mordenite.

Figure 8 shows the CN of H−ZSM-5 and H−mordenite measured during the second run. A similar pattern in the change of CN (Pd−Pd) to the first runs given in Figure 7 was observed on both H−ZSM-5 and H−mordenite. That is to say, a plateau of CN (Pd−Pd) was observed from 430 to 620 K similarly to the first run of the experiment. Therefore, it was confirmed that the generation of stable metal Pd cluster was reversible upon the oxidation with O_2 at 773 K and successive reduction with H_2. The phenomena could be feasibly understood when the fact was taken into consideration that the agglomerated metal Pd was readily redispersed onto acid sites of zeolites through the oxidation at 773 K in an O_2 flow as evidenced in section 3.1.

Figure 9 shows the change in Pd−Pd coordination number of Pd/H−mordenite plotted as a function of time after the introduction of H_2. The time-course measurement was carried out every 30 s, while the temperature of the in situ cell was kept at 723 K. After the introduction of 8% H_2 to the sample cell, a sharp increase in the Pd−Pd bond was obverted up to 1 min, suggesting that the reduction and gathering of Pd took place at the initial stage. Subsequently, the CN of metal Pd−Pd kept a constant value at 4 between 1 and 2 min. On further duration of time from 2 to 7 min, the CN(Pd−Pd) steeply increased once again. The CN of the plateau that appeared between 1 and 2 min coincided with the one observed during the temperature-programmed measurement. The data strongly indicated that the migration and coalescence of Pd progressed via the formation of Pd_6 cluster inside the pore of H−mordenite. Thus, it was noted that the selective generation of the stable Pd_6 was

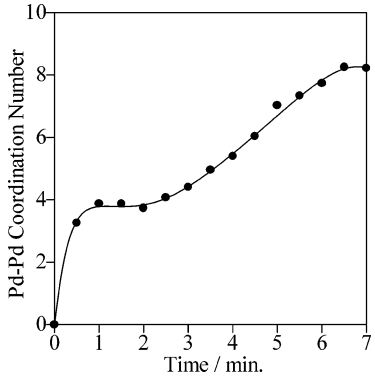

Figure 9. Time-course dependence of the coordination number of Pd−Pd (●) on Pd/H−mordenite ($Si/Al_2 = 20$) measured in an 8% H_2 flow at 723 K.

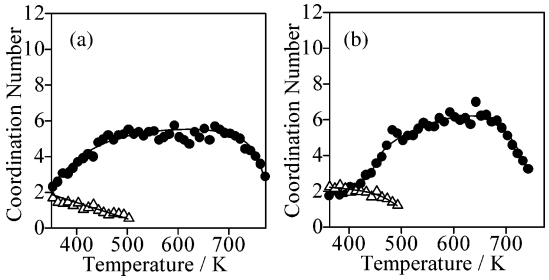

Figure 10. Dependence of the coordination number of Pd−Pd (●) and Pd−O (△) on the temperature measured in an 8% H_2 flow; (a) Pd/H−Y and (b) Pd/USY.

confirmed from the time-resolved as well as temperature-programmed measurement.

Figure 10a shows the dependence of CN on the temperature for reduction in H_2 atmosphere for Pd loaded on H−Y. In this case, the reduction of Pd oxide continued up to 500 K. At the same time the Pd−Pd of metal Pd increased, indicating the reduction of Pd oxide progressed. Then, the CN of Pd−Pd kept a constant value (5.5) up to 670 K. After the appearance of the plateau, the CN of Pd−Pd began to decrease from 670 to 770 K. The constant coordination number (CN(Pd−Pd) = 5.5) observed in H−Y was in good agreement with that of clusters with cuboctahedron structure. Therefore, the selective formation of stable Pd_{13} cluster located inside the supercage of FAU-type zeolite was inferred from the data. Although a small increase in the CN was observed between 470 and 670 K, a quite similar tendency was obverted on Pd/USY as given in Figure 10b. The slight increase in the CN between 470 and 670 K may be attributed to the structural change of clusters from cuboctahedron (CN = 5.5) to the icosahedron (CN = 6.5) or slight growth of the Pd clusters. In a manner similar to the present study, the formation of Pd carbonyl cluster with cuboctahedron structure was reported when CO was introduced to the Pd loaded on Na−Y zeolite.[21] The Pd cluster migrated from the supercage to sodalite cage or hexagonal prism with an anionic character upon the treatment at 773 K. Similarly, the reason for the decrease in the CN(Pd−Pd) observed above 670 K could be ascribed to the migration of Pd into sodalite cage or hexagonal prisms in FAU structure to generate the small Pd clusters.

In comparison with in H−ZSM-5 and H−mordenite, larger Pd clusters were stabilized in H−Y and USY zeolites. Two possibilities could be postulated to explain the difference in the generation of stable Pd clusters. The first one is that the pore structure of zeolite confined the size of clusters due to the steric confinement. However, the possibility was not plausible because similar clusters were found in H−ZSM-5 and H−mordenite, although they had different structure and pore size. In addition, the size of Pd_6 and Pd_{13} clusters was smaller than the pore size of ZSM-5 or mordenite and the supercage of Y zeolite. Another hypothesis is that the interaction between Brønsted acid sites and metal Pd determined the Pd clusters generated in zeolites in a similar manner proposed by Sachtler et al. who described the possibility of the generation of $[Pd_n\ H]^+$ adducts encaged in zeolite pores.[22,23] Actually acid strength of H−ZSM-5 or H−mordenite was higher than that of H−Y type zeolites.[24] Therefore, it could be considered that the strong acid sites anchored the small Pd_6 clusters in H−ZSM-5 and H−mordenite through the interaction between Brønsted acid sites and metal Pd.

4. Conclusions

DXAFS technique was successfully applied to follow the dispersion and clustering process of Pd in zeolites. From the measurements using different kinds of zeolites, dynamic behavior as well as the formation of various Pd clusters was revealed. In the atmosphere of oxygen, the spontaneous dispersion of PdO was observed on H−ZSM-5 and H−mordenite. In the course of the structural change, the interaction between PdO and acid sites of zeolite promoted the oxidation and subsequent dispersion of Pd. Furthermore, it was revealed that the crystal structure and acid sites of zeolites had a profound effect on the generation of stable metal Pd clusters in an atmosphere of H_2. In the case of H−ZSM-5 and H−mordenite, the formation of Pd_6 cluster was observed. The formation was repeatedly observed upon the oxidation and successive reduction with H_2. The Pd_6 cluster was also found in H−mordenite during time-resolved measurement during the course of the agglomeration. The generation of Pd_{13} cluster was obverted in H−Y and USY zeolites. In contrast with these zeolites, monotonic sintering of Pd progressed on the external surface of Na−ZSM-5 and H−β zeolites.

Acknowledgment. The synchrotron radiation experiments were performed at the BL28B2 in the SPring-8 with the approval of the Japan Synchrotron Radiation Research Institute (JASRI) (Proposal No. 2003A0492-NX -np).

References and Notes

(1) Weber, W. A.; Gates, B. C. *J. Catal.* **1998**, *180*, 207.
(2) Brabec, L.; Nováková, J. *J. Mol. Catal. A* **2001**, *166*, 28.
(3) Gurin, V. S.; Petranovskii, V. P.; Bogdanchikova, N. E. *Mater. Sci. Eng.* **2002**, *C19*, 327.
(4) Jacobs, G.; Ghadiali, F.; Posanu, A.; Borgna, A.; Alvarez, W. E.; Resasco, D. E. *Appl. Catal. A* **1999**, *188*, 79.
(5) Wen, B.; Sun, Q.; Sachtler, W. M. H. *J. Catal.* **2001**, *204*, 314.
(6) Gélin, P.; Primet, M. *Appl. Catal. B* **2002**, *39*, 1.
(7) Chin, Y. H.; Resasco, D. E. *Catalysis*, Vol. 14; Royal Society of Chemistry: London, 1998.
(8) Nishizaka, Y.; Misono, M. *Chem. Lett.* **1993**, 1295.
(9) Mehnert, C. M.; Weaver, D. W.; Ying, J. Y. *J. Am. Chem. Soc.* **1998**, *120*, 12289.
(10) Moller, K.; Koningsberger, D. C.; Bein, T. *J. Phys. Chem.* **1989**, *93*, 6116.
(11) Bergeret, G.; Gallezot, P.; Imelik, B. *J. Phys. Chem.* **1981**, *85*, 411.
(12) Okumura, K.; Amano, J.; Niwa, M. *Chem. Lett.* **1999**, 997.
(13) Okumura, K.; Amano, J.; Yasunobu, N.; Niwa, M. *J. Phys. Chem. B* **2000**, *104*, 1050.
(14) Okumura, K.; Niwa, M. *Catal. Surv. Jpn.* **2002**, *5*, 121.
(15) Okumura, K.; Niwa, M. *J. Phys. Chem. B* **2000**, *104*, 9670.
(16) Neylon, M. K.; Marshall, C. L.; Kropf, A. J. *J. Am. Chem. Soc.* **2002**, *124*, 5457.
(17) Okumura, K.; Kusakabe, T.; Yokota, S.; Kato, K.; Tanida, H.; Uruga, T.; Niwa, M. *Chem. Lett.* **2003**, *32*, 636.
(18) Okumura, K.; Yoshimoto, R.; Yokota, S.; Kato, K.; Tanida, H.; Uruga, T.; Niwa, M. *Phys. Scr.*, in press.

(19) Van Zon, J. B.; Koningsberger, D. C.; Van Blik, H. F. J.; Sayers, D. E. *J. Phys. Chem.* **1985**, *82*, 5742.

(20) Guillemot, D.; Polisset-Thfoin, M.; Fraissard, J. *J. Phys. Chem. B* **1997**, *101*, 8243.

(21) Zhang, Z.; Huaiyu, C.; Sheu, L.-L.; Sachtler, W. M. H. *J. Catal.* **1991**, *127*, 213.

(22) Bai, X.; Sachtler, W. M. H. *J. Catal.* **1991**, *129*, 121.

(23) Homeyer, S. T.; Kapinski, Z.; Sachtler, W. M. H. *J. Catal.* **1990**, *123*, 60.

(24) Katada, N.; Igi, H.; Kim, J.-H.; Niwa, M. *J. Phys. Chem. B* **1997**, *101*, 5659.